Title

Effect of cigarette smoking on nitric oxide, structural, and mechanical properties of mouse arteries

Journal

AJP Heart and Circulatory Physiology, 291(5)

ISSN

0363-6135

Authors

Guo, X
Oldham, MJ
Kleinman, MT
et al.

Publication Date

2006-11-01

DOI

10.1152/ajpheart.00376.2006

Am J Physiol Heart Circ Physiol 291: H2354–H2361, 2006.
First published June 30, 2006; doi:10.1152/ajpheart.00376.2006.

Effect of cigarette smoking on nitric oxide, structural, and mechanical properties of mouse arteries

X. Guo,[1] M. J. Oldham,[4] M. T. Kleinman,[4] R. F. Phalen,[4] and G. S. Kassab[1,2,3]

Departments of [1]Biomedical Engineering, [2]Surgery, and [3]Cellular and Integrative Physiology, Indiana University Purdue University Indianapolis, Indianapolis, Indiana; and [4]Department of Community and Environmental Medicine, University of California, Irvine, California

Submitted 8 April 2006; accepted in final form 14 June 2006

Guo, X., M. J. Oldham, M. T. Kleinman, R. F. Phalen, and G. S. Kassab. Effect of cigarette smoking on nitric oxide, structural, and mechanical properties of mouse arteries. *Am J Physiol Heart Circ Physiol* 291: H2354–H2361, 2006. First published June 30, 2006; doi:10.1152/ajpheart.00376.2006.—Cigarette smoking (CS) is a major risk factor for vascular disease. The aim of this study was to quantitatively assess the influence of CS on mouse arteries. We studied the effect of short-term (6 wk) and long-term (16 wk) CS exposure on structural and mechanical properties of coronary arteries compared with that of control mice. We also examined the reversibility of the deleterious effects of CS on structural [e.g., wall thickness (WT)], mechanical (e.g., stiffness), and biochemical [e.g., nitric oxide (NO) by-products] properties with the cessation of CS. The left and right coronary arteries were cannulated in situ and mechanically distended. The stress, strain, elastic modulus, and WT of coronary arteries were determined. Western blot analysis was used to analyze endothelial NO synthase (eNOS) in the femoral and carotid arteries of the same mice, and NO by-products were determined by measuring the levels of nitrite. Our results show that the mean arterial pressure was increased by CS. Furthermore, CS significantly increased the elastic modulus, decreased stress and strain, and increased the WT and WT-to-radius ratio compared with those of control mice. The reduction of eNOS protein expression was found only after long-term CS exposure. Moreover, the NO metabolite was markedly decreased in CS mice after short- and long-term exposure of CS. These findings suggest that 16 wk of CS exposure can cause an irreversible deterioration of structural and elastic properties of mouse coronary arteries. The decrease in endothelium-derived NO in CS mice was seen to significantly correlate with the remodeling of arterial wall.

nitrite; strain; stress; elastic modulus; stiffness

SUBSTANTIAL EPIDEMIOLOGICAL evidence indicates an association between cigarette smoking (CS) and cardiovascular disease, in particular atherosclerosis (15, 20). It has been shown that exposure to CS increases myocardial oxygen demand (17) and concurrently reduces coronary blood flow by causing vasoconstriction in the coronary arteries and microvasculature (3). The mechanism for the increased risk of vascular dysfunction is not well understood, but it is presumed to be due to the absorption of tobacco smoke constituents that affect endothelial cell function (17, 26).

Nitric oxide (NO) is an endothelium-derived relaxing factor synthesized in arterial endothelium from the amino acid L-arginine by the enzyme NO synthase (NOS), which is expressed constitutively in endothelial cells (eNOS or type III NOS) (24). Endothelium-derived NO is a potent endogenous vasodilator that contributes to resting arterial tone and affects both platelet function and smooth muscle cell proliferation (28). The eNOS is essential in maintaining basal vascular NO production that regulates blood flow, particularly coronary blood flow. Reduction in basal NO release may cause a predisposition to hypertension, thrombosis, vasospasm, and atherosclerosis (25). In vivo, CS (34) and nicotine infusion (4) impair the endothelium-dependent relaxation mediated by NO in human arteries and veins.

Arterial mechanical properties can be influenced by several factors, such as heart rate, atherosclerotic plaque, blood pressure, and age. Houdi et al. (13) found that the exposure of conscious rats to CS resulted in a decrease in heart rate and cardiac output and an increase in mean arterial pressure and total peripheral resistance. Previous studies (18) have shown that acute CS decreased arterial compliance in both large elastic and medium-sized muscular arteries. An invasive study (29) in men with coronary artery disease has shown that acute exposure to passive smoking impairs elastic properties of the aorta. Although these past studies have established that CS causes changes in the coronary blood vessels and circulation, no systematic data on the remodeling of the mouse coronary arteries exist nor have the changes been correlated with the NO bioavailability.

The present study was designed to determine the effects of short-term (6 wk) and long-term (16 wk) CS exposure on the structural and biomechanical properties of the coronary arteries. Furthermore, the reversibility of the deleterious remodeling after CS cessation was also addressed. We hypothesized that NO derived from endothelium is intimately connected with arterial wall structure and mechanical properties. In conjunction with the changes in the mechanical properties of coronary arteries, we assessed the effect of CS on basal NO production (nitrite and nitrate) and eNOS protein expression in the vessel wall. Our findings confirm a correlation between NO and the change of structural and mechanical status of arterial wall in response to CS.

METHODS

Cigarette Smoke Exposure

Forty-two homozygous, inbred male mice (C57BL/6 strain) were used in this study. The Walton Smoke Exposure Machine (Process & Instruments, Brooklyn, NY) was used to puff 1R3 cigarettes according to the Federal Trade Commission puffing regimen (35 ml over 2 s;

Address for reprint requests and other correspondence: G. S. Kassab, Dept. of Biomedical Engineering, SL-174, Indiana Univ. Purdue Univ. Indianapolis, 723 W. Michigan St., Indianapolis, IN 46202 (e-mail: gkassab@iupui.edu).

The costs of publication of this article were defrayed in part by the payment of page charges. The article must therefore be hereby marked "*advertisement*" in accordance with 18 U.S.C. Section 1734 solely to indicate this fact.

1 puff/min) to generate the mainstream smoke used for exposure of mice in this study. The machine was operated to deliver a 1-day exposure equivalent to that of 1 pack per day for a human smoker. Adjusting for the difference in ventilation per unit body mass of the mouse and human, a 4-h exposure to 24 cigarettes was selected. Mice were exposed to mainstream cigarette smoke via nose-only exposure manifold (Intox Products, Moriaty, NM) at age 8 or 9 wk. This exposure was performed daily (5 days/wk). The mice were divided into two groups according to the duration of CS exposure that included controls (filter-air, nose-only exposure), CS exposure (CS), and CS exposure + recovery (CS + RE). In the first group, 12 mice were exposed to the smoke of the 1R3 commercial cigarettes (University of Kentucky) 4 h per day for 6 wk, and six of these mice were euthanized at the day of cessation of smoke exposure. The remaining six mice were then returned to the air exposure for 3 wk (CS6 + RE3). Five mice and six mice were used as sham controls for the CS and CS6 + RE3 subgroups, respectively. In the second group, 10 mice were exposed to the CS for 16 wk, and five of these mice were euthanized at the day of cessation of smoke exposure. The remaining five mice were then returned to the air exposure for 8 wk after 16 wk of smoke exposure (CS16 + RE8). Five and four mice were used as sham controls for the CS and CS16 + RE8 subgroups, respectively. The control mice were restrained daily (5 days/wk) in the smoking machine (filter-air, nose-only exposure) for the identical duration of time with the experimental groups to mimic the restraint and environmental stress of the smoking machine. The mean body weight and age of each group are listed in Table 1.

Animal Preparation

The mice were anesthetized with intraperitoneal injections of ketamine (80 mg/kg) and xylazine (8 mg/kg). Arterial blood pressure was measured by inserting a catheter into the common carotid artery connected to a pressure transducer. Heparin (200 U/ml) was used to prevent blood clots in the vessels via the carotid artery catheter. All animal experiments were performed in accordance with national and local ethical guidelines, including the Institute of Laboratory Animal Research Guide, Public Health Service policy, Animal Welfare Act, and were approved by the Institutional Animal Care and Use Committee of the University of California, Irvine.

Nitrite/Nitrate Measurements

The mouse was euthanized with an overdose of ketamine and xylazine via the jugular vein. The left femoral and carotid arteries were isolated immediately and were coarsely grounded in methanol in an ice bath. Homogenate (~50 μl in total volume) was centrifuged at 800 *g* at 4°C for 10 min, and the supernatant was then assayed for nitrite (NO_2^-) and nitrate (NO_3^-). The nitrite and nitrate ion concentrations in solution were measured by the combination of a diazo-coupling method and high-performance liquid chromatography (ENO-20 NO_x Analyser; EiCom, Kyoto, Japan). The method for NO_x analysis has been previously described in detail (23). Briefly, the peaks of detected voltage for nitrite and nitrate were converted into nitrite and nitrate concentrations by the use of calibration solutions. The signals were corrected for contamination by subtraction of the control nitrite concentration. The endogeneous NO production was evaluated as the concentration of nitrite or nitrate per unit volume of arterial wall (in nmol/mm^3).

In five control mice, the carotid, femoral, left coronary artery (LCA), and right coronary artery (RCA) were harvested, and the NO_x concentrations were determined. This was done to establish a correlation between the NO_x in the coronary and femoral and carotid arteries, because it is not possible to make both mechanical and biochemical measurements on the same vessels.

Table 1. *Body weight and age for control, CS, and CS + RE mice.*

Group	Weight, g	Age, wk	*n*
CS-6 wk	22.6±1.1	14.7±0.5	6
Control for CS-6 wk	22.5±1.9	14.2±1.1	5
CS6 + RE3	23.8±1.6	18.8±0.7	6
Control for CS6 + RE3	25.2±1.0	20.3±1.5	6
CS-16 wk	24.4±1.7	24.5±0.7	5
Control for CS-16 wk	24.7±2.0	25.2±0.9	5
CS16 + RE8	25.0±0.9	32.1±0.9	5
Control for CS16 + RE8	27.6±1.6	33.0±0.8	4

Values are means ± SD; *n,* number of mice. CS6 + RE3 group, 6 wk of cigarette smoke (CS) exposure, followed by 3 wk of recovery (RE); CS16 + RE8 group, 16 wk of CS exposure, followed by 8 wk of RE.

Western Blot Analysis

The right femoral and carotid artery were removed and homogenized in a lysis buffer containing 50 mmol/l β-glycerophosphate, 100 μmol/l sodium orthovanadate, 2 mmol/l magnesium chloride, 1 mmol/l EGTA, 0.5% Triton X-100, 1 mmol/l *dl*-dithiothreitol, 20 μmol/l pepstatin, 20 μmol/l leupeptin, 0.1 U/ml aprotinin, and 1 mmol/l phenylmethylsulfonyl fluoride and then incubated on ice for 1 h. The sample was centrifuged at 1,000 *g* for 15 min at 1°C, and the supernatant was collected. The total protein was measured by BCA kit (Bio-Rad). Equal amounts of protein (25 μg) were loaded and electrophoresed in a 10% SDS-PAGE gel and transferred onto a ployvinylidene difluoride membrane. After being blocked for 2 h in 8% dried milk in Tris-buffered saline-Tween buffer, the membrane was incubated overnight at 4°C with specific primary antibody (1:1,000 dilution in blocking buffer, BD Transduction). The membrane was then rinsed and incubated with horseradish peroxidase-conjugated secondary antibody for 2 h (1:3,000 dilution in blocking buffer, Bio-Rad). Specific eNOS protein was detected by enhanced chemiluminescence (Amersham Biosciences) and evaluated by densitometry (SigmaScan, Systat Software). All samples from each group were simultaneously probed with anti-β-actin, a mouse monoclonal antibody (primary antibody 1:1,000 dilution in blocking buffer, Santa Cruz Biotechnololgy) to correct for sample loading. Positive control protein was obtained from cultured human vascular endothelial cells provided by BD Transduction.

Mechanical Testing: Pressure-Diameter-Length Relation

The heart was immediately excised and placed in a Krebs solution after the mouse was euthanized. The anterior portion of the main trunk of the LCA and RCA close to the opening of the aorta was then exposed carefully. Water-insoluble carbon particles were used to mark the segment of the main trunk of the LCA and RCA (~0.5–0.6 mm in length) to measure axial-length changes. The ascending aorta was then cannulated by a 23-gauge needle and perfused with 6% dextran solution at the various perfusion pressures. Cab-O-Sil (0.35% by weight), a colloidal silica, was mixed into the dextran solution to prevent flow through the microvessels and, hence, to attain zero-flow distensions. The LCA and RCA were preconditioned with five cyclic changes in pressure from 0 to 150 mmHg in a triangular waveform. The pressure was increased in 30-mmHg step increments from 30 to 150 mmHg in a staircase manner. The external geometry of the LCA and RCA segment, at the pressurized state, was photographed at ×100 magnification to obtain the loaded outer diameter and the in vivo axial length.

No-load and Zero-Stress State

After the mechanical testing was completed, the marked blood vessel segment of the LCA and RCA were carefully dissected and placed into a Ca^{2+}-free Krebs solution, aerated with 95% O_2-5% CO_2.

The vessel segment was then cut transversely into five or six rings. Each ring was photographed at ×100 magnification in no-load state (zero transmural pressure) and then cut radially by a scissor to reveal the zero-stress state. The ring opened into a sector and gradually approached a constant opening angle. The cross section of each sector was photographed 1 h after the radial cut. The morphological measurements of the in vitro axial length, inner and outer circumference, wall thickness (WT), and area in the no-load and zero-stress state were made from the images using a morphometric analysis system (SigmaScan).

Biomechanical Analysis

Incompressibility condition. The loaded inner radius and WT of vessel were determined from the incompressibility assumption. The incompressibility condition for a cylindrical vessel can be expressed as follows:

$$r_i = \sqrt{r_o^2 - \frac{A_o}{\pi\lambda_z}} \quad (1a)$$

where r_o and r_i are the outer and inner radii at the loaded state, respectively; λ_z is l/l_o as the stretch ratio in the axial direction where l and l_o are the vessel length in the loaded and zero-stress state, respectively; and A_o is the wall area in the no-load state. WT, at the loaded state, was computed as the difference between the outer and inner radius of the vessel at various pressures as follows:

$$WT = r_o - r_i = r_o - \sqrt{r_o^2 - \frac{A_o}{\pi\lambda_z}} \quad (1b)$$

where r_o, A_o, and λ_z were measured quantities.

Strain and stress. The circumferential deformation of the artery may be described by Green strain, ε_θ, which is defined as follows:

$$\varepsilon_\theta = \frac{1}{2}[\lambda_\theta^2 - 1] \quad (2)$$

where λ_θ is the midwall circumferential stretch ratio ($\lambda_\theta = c/c^{zs}$), c refers to the midwall circumference of the vessel in the loaded or no-load state, and c^{zs} refers to the midwall circumference in the zero-stress state.

At equilibrium, the average circumferential Cauchy and second Piola-Kirchoff stress in a cylinder can be computed as follows:

$$\tau_\theta = \frac{Pr_i}{WT} \quad (3a)$$

and

$$S_\theta = \frac{\tau_\theta}{\lambda_\theta^2} \quad (3b)$$

where P is the luminal pressure and r_i and λ_θ are the inner radius and the circumferential stretch ratio of the vessel, respectively. *Equations 2* and *3* allow the determination of the circumferential stresses and strains, respectively, for different pressure distensions.

Elastic moduli. The computation of elastic modulus has been previously described in detail (10). In analogy to an isotropic tube, the circumferential elastic modulus (E_θ) can be defined as:

$$E_\theta = \frac{\frac{\Delta\tau_\theta}{\Delta\varepsilon_\theta}}{\left[1 - \frac{\Delta\tau_z}{\Delta\varepsilon_z}\frac{1}{E_z}\right]} \quad (4a)$$

where

$$E_z = \frac{\Delta\tau_z}{\Delta\varepsilon_z} + \left(\frac{\Delta\varepsilon_\theta}{\Delta\varepsilon_z}\right)^2 \frac{\Delta\tau_\theta}{\Delta\varepsilon_\theta} \quad (4b)$$

Because the stress-strain relation was found to be linear, E_θ and E_z are constant and independent of pressure.

Statistical Analysis

All values for mechanical analysis and quantitative analysis for Western blot analysis were expressed as means ± SD, expect for NO by-product (nitrite) measurements that were expressed as means ± SE. Significance of the differences between the different groups were evaluated by two-way ANOVA or *t*-test. The results were considered statistically significant when $P < 0.05$ (2-tailed).

RESULTS

There were no significant differences between control mice for CS and control mice for CS + RE, so the various parameters of CS and CS + RE control groups were combined. Mean carotid arterial pressures for control, CS, and CS + RE mice after 6 and 16 wk of CS exposure are shown in Fig. 1. The arterial pressures were significantly affected by CS compared with those of control mice ($P < 0.05$). There was no significant difference in blood pressure between mice treated with 6 wk of CS followed by 3 wk of recovery (CS6 + RE3) and control mice. However, the arterial pressure was found to be still higher in mice treated with 16 wk of CS followed by 8 wk of recovery (CS16 + RE8) compared with that of control mice ($P < 0.05$).

All measurements were made in duplicate, and the mean was reported. The NO concentration was measured as nitrite, a stable degradation by-product of NO. Figure 2*A* shows the NO concentration of femoral and carotid arteries for control, CS, and CS + RE mice after 6 and 16 wk of smoke exposure. The NO concentration was significantly reduced in CS and CS + RE mice after 16 wk of smoke exposure compared with that of control mice ($P < 0.01$). For the mice after 6 wk of smoke exposure, we found the NO concentration was significantly decreased in CS mice compared with that of control mice ($P = 0.04$), which was not significantly different from that of CS + RE mice. Figure 2*B* shows the relationships between mean arterial pressure and nitrite concentration of femoral and carotid artery for all the mice. There was a negative correlation between arterial pressure and nitrite concentration ($P < 0.01$).

A positive correlation was found between the NO production of coronary arteries with those of femoral and carotid arteries ($Y = 3.33X - 0.53$, $R^2 = 0.79$, $P < 0.05$, where Y and X

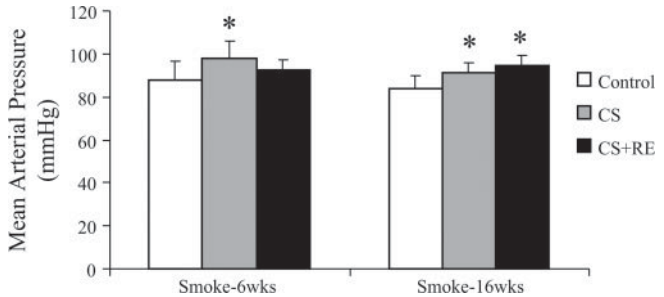

Fig. 1. Mean arterial pressure for control, cigarette smoke (CS), and smoke recovery (CS + RE) mice after 6 and 16 wk of smoke exposure. *$P < 0.05$, when CS or CS + RE mice were compared with control.

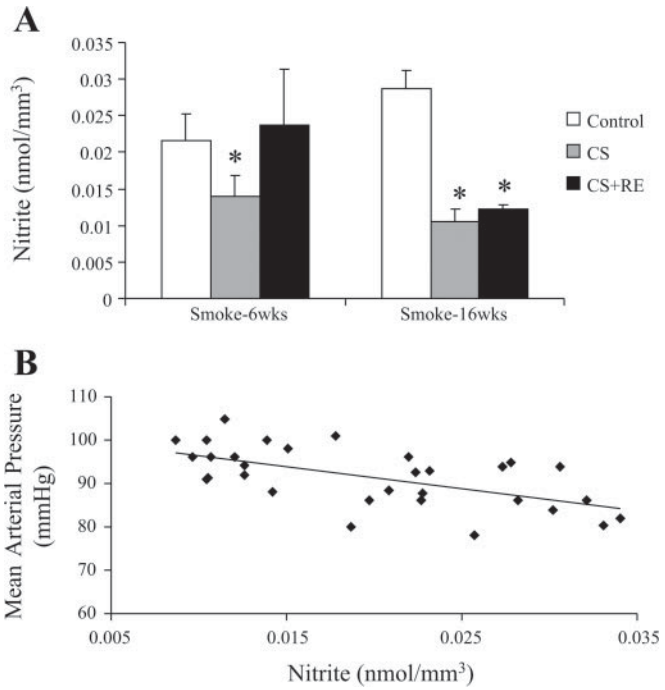

Fig. 2. *A*: nitric oxide (NO) by-product (nitrite) concentration of femoral and carotid artery for control, CS, and CS + RE mice after 6 and 16 wk of smoke exposure. *$P < 0.05$, when CS or CS + RE mice were compared with control. *B*: relationship between mean arterial pressure (P) and nitrite concentration (N) of femoral and carotid artery for all mice. A linear least-square fit is used to fit data as $P = -515.1N + 101.7$ ($R^2 = 0.37$, $P < 0.01$).

represent nitrite concentration of coronary arteries and combined femoral and carotid arteries, respectively).

Figure 3 shows Western blot and quantitative analysis of eNOS protein expression in the femoral and carotid artery for control, CS, and CS + RE mice after 6 and 16 wk of smoke exposure. A band at 140 kDa was detected, which was similar in size with the band for human endothelium cell protein standard. The anti-β-actin antibody reacted with a 42-kDa protein corresponding to the size of β-actin. The final value for eNOS densitometry was computed as the ratio of eNOS to β-actin. The CS and CS + RE group did not differ from the control in eNOS protein expression after 6 wk of CS exposure. The eNOS protein expression of femoral and carotid artery was significantly lower in CS than in control mice ($P < 0.05$) after 16 wk of smoking exposure. There was no significant difference in eNOS protein expression between CS16 + RE8 and control mice.

The inner diameter and the WT (intima-media) of LCA and RCA were computed according to *Eqs. 1a* and *1b* based on the incompressibility assumption. As expected, the inner diameter increased ($P < 0.001$), whereas the WT decreased ($P < 0.001$) with an increase in perfusion pressure (data not shown). Figure 4 shows the WT of LCA and RCA and the WT-to-radius (WTTR) ratio of LCA and RCA for control, CS, and CS + RE mice at physiological pressure (120 mmHg) after 6 and 16 wk of CS exposure. The data of WTTR ratio of LCA and RCA were combined because there were no statistically significant differences between them. The WT of LCA was significantly increased after 6 wk of CS exposure compared with that of control mice ($P < 0.01$), which was not significantly different from that of CS6 + RE3 mice. The WT of LCA in CS mice at

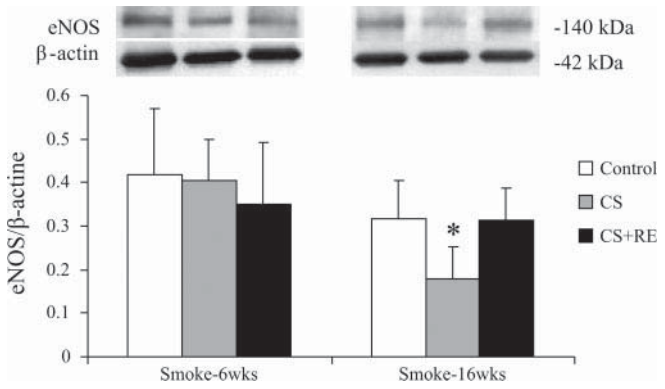

Fig. 3. Western blot and quantitative analysis of endothelial NO synthase (eNOS) protein expression of the femoral and carotid artery for control, CS, and CS + RE mice after 6 and 16 wk of smoke exposure. *$P < 0.05$, when CS or CS + RE mice were compared with control.

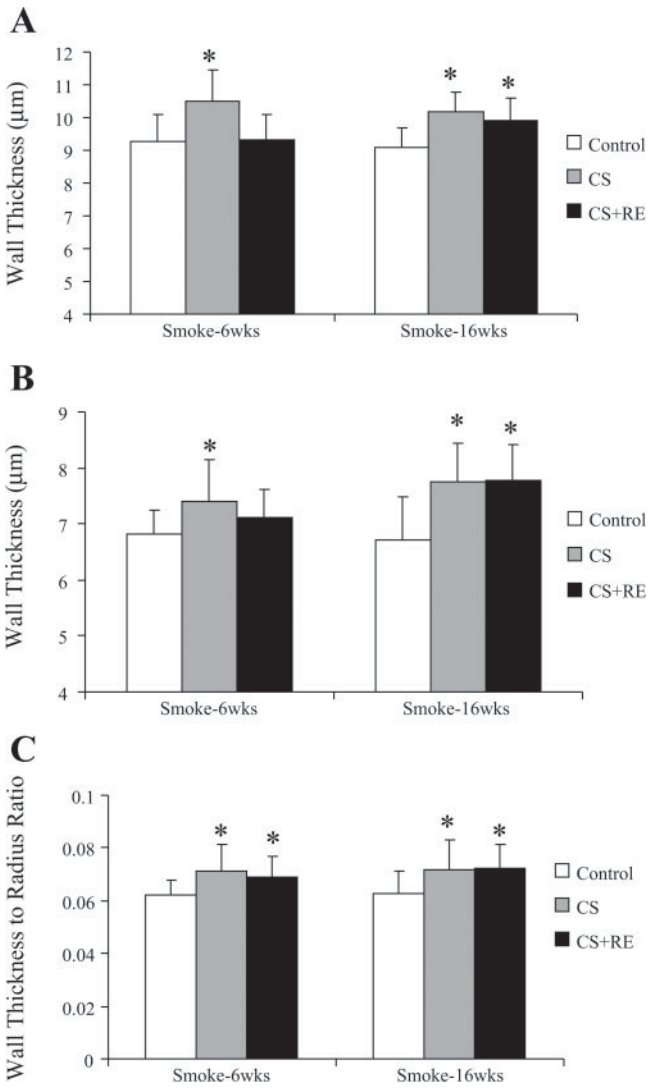

Fig. 4. Wall thickness of left coronary artery (LCA; *A*) and right coronary artery (RCA; *B*) and wall thickness-to-radius ratio of LCA and RCA (*C*) for control, CS, and CS + RE mice at physiological pressure (120 mmHg) after 6 and 16 wk of smoke exposure. *$P < 0.05$, when CS or CS + RE mice were compared with control.

16 wk and CS16 + RE8 mice showed a significant increase compared with that of control mice ($P < 0.01$). Similar results were found for the RCA ($P < 0.05$). For the WTTR ratio, a significant increase was observed in both CS and CS + RE mice after 6 and 16 wk of CS exposure compared with that of control mice ($P < 0.05$).

The midwall Green strain and mean Cauchy stress of LCA and RCA for control, CS, and CS + RE mice at physiological pressure (120 mmHg) after 6 and 16 wk of smoke exposure are shown in Fig. 5. There was no significant difference for Green strain and Cauchy stress between LCA and RCA, so the data of LCA and RCA were combined. The midwall Green strain and mean Cauchy stress of LCA + RCA were significantly decreased in CS and CS + RE mice after both 6 and 16 wk of smoke exposure compared with those of control mice ($P < 0.05$).

The relationship between Green strain and second Piola-Kirchhoff stress of the LCA and RCA in CS, CS + RE, and control mice were found to be linear ($R^2 > 0.95$). The circumferential elastic modulus was computed using *Eqs. 4a* and *4b*. Figure 6 shows the circumferential elastic modulus of LCA for control, CS, and CS + RE mice after 6 and 16 wk of smoke exposure. The circumferential modulus of the LCA was significantly larger in mice treated with 6 wk of CS than in control mice ($P < 0.01$). But there was no significant difference for the circumferential modulus between CS6 + RE3 and control mice. For the mice at 16 wk of smoke exposure, the circumferential modulus of LCA was significantly increased both in CS and CS16 + RE8 mice compared with that of the respective control mice ($P < 0.05$). Similar results were observed for the RCA (data not shown).

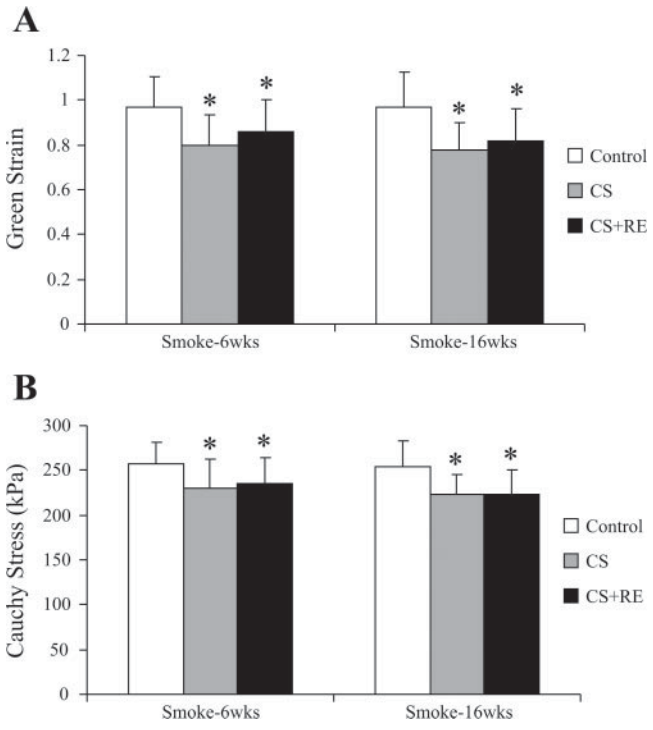

Fig. 5. Midwall Green strain (*A*) and mean Cauchy stress (*B*) of LCA and RCA for control, CS, and CS + RE mice at physiological pressure (120 mmHg) after 6 and 16 wk of smoke exposure. *$P < 0.05$, when CS or CS + RE mice were compared with control.

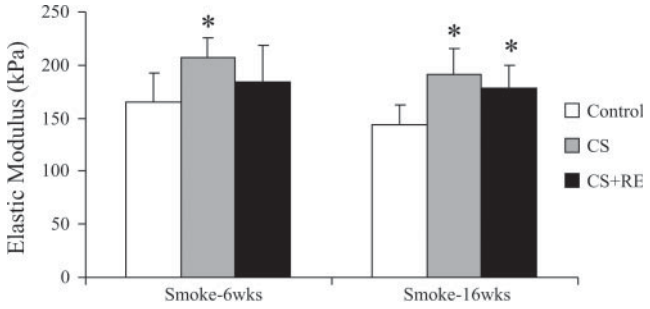

Fig. 6. Circumferential elastic modulus of LCA for control, CS, and CS + RE mice after 6 and 16 wk of smoke exposure. *$P < 0.05$, when CS or CS + RE mice were compared with control. Data are means ± SD.

The open sector in the zero-stress state was characterized by the opening angle, which was defined as the angle subtended by two radii connecting the midpoint of the inner wall to the ends of the open segment. The opening angles of combined LCA and RCA data (no significant difference between LCA and RCA) for control, CS, and CS + RE mice after 6 and 16 wk of smoke exposure are shown in Fig. 7. No significant changes in opening angle were found in CS and CS + RE mice after 6 wk of smoking exposure compared with those of control mice. A significant decrease in opening angle was seen, however, in CS and CS + RE mice compared with that of control after 16 wk of CS exposure ($P < 0.05$).

The relationships between coronary WT, Green strain, Cauchy stress, and elastic modulus and nitrite concentration of femoral and carotid artery at a pressure of 120 mmHg for all the mice are shown in Fig. 8. The Green strain and Cauchy stress increase linearly with an increase in nitrite ($P < 0.01$), as shown in Fig. 8, *B* and *C*, respectively. The WT and elastic modulus decrease linearly with an increase in nitrite ($P < 0.01$), as shown in Fig. 8, *A* and *D*, respectively. The data were fitted by a linear least-square fit, and the empirical constants are summarized in Fig. 8.

DISCUSSION

Blood Pressure

There are several interacting homeostatic regulators of blood pressure, including the rennin-angiotensin system, the autonomic nervous system, and local mediators. The myogenic tone and flow-dependent vasodilation are of major importance for the regulation of blood pressure under various physiological circumstances. Some studies (8) have shown that CS is

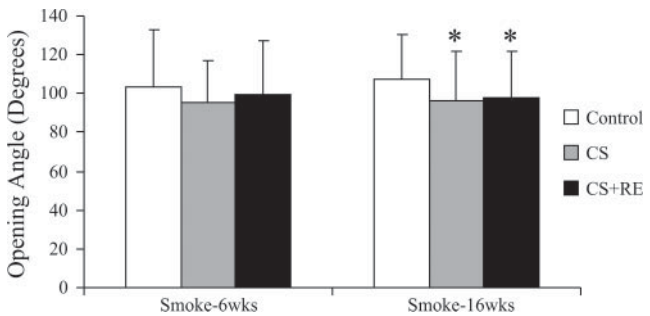

Fig. 7. Opening angle of LCA and RCA for control, CS, and CS + RE mice after 6 and 16 wk of smoke exposure. *$P < 0.05$, when CS or CS + RE mice were compared with control.

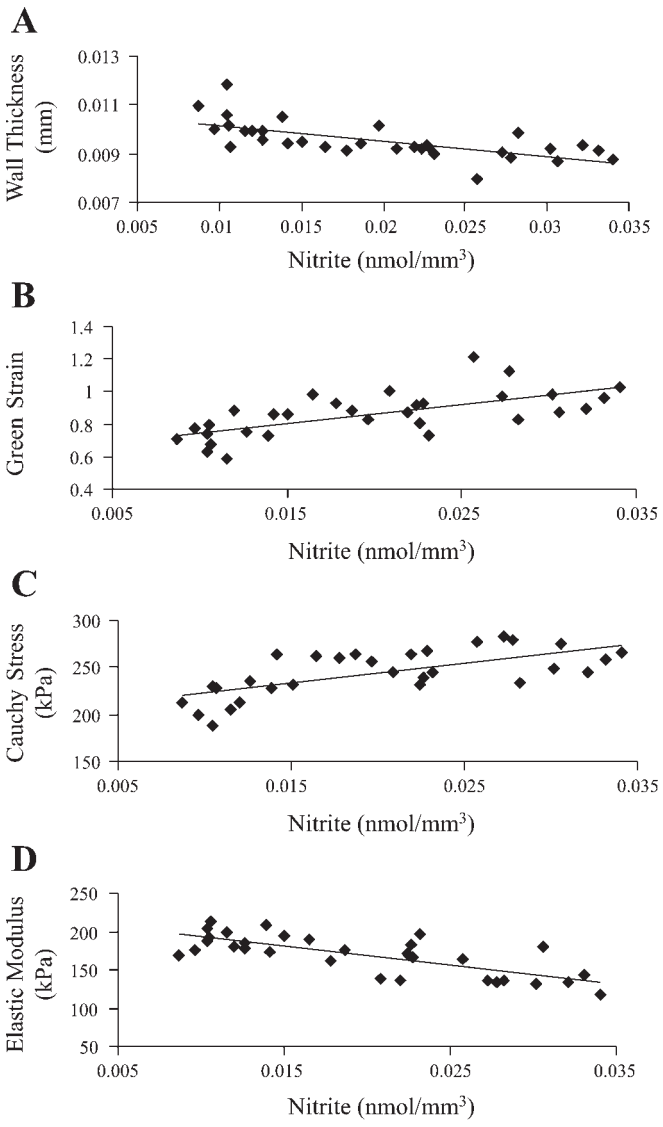

Fig. 8. Relationship between wall thickness (*A*), Green strain (ε; *B*), Cauchy stress (τ; *C*), elastic modulus (*E*; *D*) and concentration of nitrite (N) at pressure of 120 mmHg for all mice. A linear least-square fit is used to fit data as follows: wall thickness = $-6.2E-03N + 0.01$ ($R^2 = 0.45$, $P < 0.01$); $\varepsilon = 11.6N + 0.6$ ($R^2 = 0.44$, $P < 0.01$); $\tau = 2099.9N + 202.3$ ($R^2 = 0.45$, $P < 0.01$); $E = -2432.8N + 216.9$ ($R^2 = 0.56$, $P < 0.01$).

associated with an acute and marked increase in blood pressure and heart rate. This study shows that CS increases the blood pressure of mouse, as shown in Fig. 1. It is well known that NO is a vasodilator released by the endothelium in response to flow or shear stress. NO has been associated with the regulation of blood pressure and regional blood flow (14). Rees et al. (27) found that the pharmacological blockage of NO synthesis induced a dose-dependent, long-lasting increase in mean systemic arterial blood pressure. Our data confirmed that the NO bioavailability was significantly decreased by CS (Fig. 2*A*). Furthermore, a negative linear relation between NO production (nitrite) of femoral and carotid artery and blood pressure was observed (Fig. 2*B*). Although regulation of blood pressure occurs primarily by resistance-size arteries, these data on epicardial (150–200 μm in diameter) arteries show that the increase of the mean arterial pressure of mouse in response to CS correlates with vascular NO.

NO Production and eNOS Protein Expression

The association between CS and vascular diseases is widely recognized, and there is a general consensus that CS targets the vascular endothelial cells. Endothelial integrity is essential for homeostatic function of blood vessels and for maintaining a nonthrombotic and nonatherogenic state. NO is a potent vasodilator that inhibits extracellular matrix turnover and can thus modify the mechanical properties of the arterial wall (33). Higman et al. (11) reported that the release of NO from saphenous veins of nonsmokers was significantly higher than that from veins of heavy smokers. Using the NO antagonist N^G-monomethyl-L-arginine, several investigators (19) have found indirect impairment of endothelium-dependent vasodilatation in smokers with decreased NO. In the present study, the measurement of nitrite (aqueous oxidation products of NO) from femoral and carotid artery after short-term and long-term CS exposure provides evidence that CS significantly decreases the bioavaibility of NO. Furthermore, the impaired release of endothelial NO was reversible for mice at 3 wk after cessation of short-term exposure of CS (Fig. 2).

Impaired release of endothelial NO is thought to be related to the reduced synthesis or activity of eNOS (11). Recently, both an increase and a decrease of eNOS mRNA and protein have been reported in relation to the effect of cigarette smoke in various experimental models. CS has been shown to inhibit pulmonary artery eNOS (31) and to suppress eNOS by ~52% in cultured endothelial cells (35). Conversely, Barua et al. (2) found a higher eNOS expression in human umbilical vein endothelial cells treated with serum from smokers. To date, the changes in protein expression of eNOS of mouse coronary arteries have not been documented. The present data show that eNOS protein expression is markedly affected only by long-term, but not by short-term, CS exposure. Moreover, the decrease of eNOS protein expression was reversed after cessation of smoke for 8 wk after 16 wk of CS exposure (Fig. 3). It has been reported that CS contains a variety of oxidants, including nitrogen oxides, hydrogen peroxide, hydrogen cyanide, and acrolein (12), that are capable of affecting eNOS expression. In the present study, the protein expression of eNOS appears to be a less sensitive biomarker for the structural and mechanical remodeling of coronary artery than the NO concentration. Future studies should investigate the activity of eNOS as a biomarker. Furthermore, the role of increased reactive oxygen species as a cause of decreased NO bioavailability in this model warrants attention. Finally, other enzymes responsible for NO synthesis, such as inducible NOS and neuronal NOS, should also be investigated.

Structural Properties

Intimal-medial WT has emerged as an index of cardiovascular disease and is generally regarded as a biomarker of atherosclerosis. The study by Auerbach et al. (1) has shown qualitatively that smokers have an unusual hyaline thickening of the arterioles that are rare in nonsmokers. A study in mice found that after 5 wk of exposure to CS, the carotid intimal area was significantly increased in the exposure group (32). Our data showed an increase in WT (intima-media) and WTTR

ratio of the coronary wall after CS exposure (Fig. 4), which may predispose the coronary arteries to atherosclerosis.

The WTTR ratio was not restored to control value in either recovery group. The effect of short-term exposure to CS on the WT, however, was reversible after the cessation of CS exposure. This is likely due to the restoration of NO bioavailability that can reduce hyperplasia. Moreover, we found that mean arterial pressure was increased by ~8% to 10% and that WTTR ratio was increased by ~13 to 14% after 6 and 16 wk of CS exposure. This suggests that the increase in WTTR ratio may be partly due to the blood pressure and partly due to the biochemical affect of CS (decrease in NO bioavailability).

Mechanical Properties

Arterial stiffness is recognized as an important cardiovascular risk factor and an independent predictor of all-cause and cardiovascular death. Hence, a number of studies have focused on the changes in mechanical properties of blood vessels in response to CS. Liu and Fung (21) studied the effect of CS (2 and 3 mo) on the mechanical properties of the pulmonary arteries of the rat. They found an increase in the stiffness of the pulmonary arteries in smoke-exposed rats. Kool et al. (18), using noninvasive methodology in smokers, showed an acute decrease in the distensibility of both elastic common carotid artery and muscular brachial artery. There are no similar data on the coronary arteries, which are very susceptible to the effects of CS. Our results indicate that CS significantly increases the circumferential elastic modulus of coronary arteries, suggesting an increase in arterial stiffness (Fig. 6). We also found the elastic modulus to be restored to the normal value after 6 wk of CS exposure, whereas it remained larger than the control value after 16 wk of CS exposure. These findings underscore the relation between reversibility of the changes in mechanical properties and the dose of CS.

The zero-stress state of a blood vessel is an open sector that is quantified by the opening angle. The remodeling of the zero-stress state is an index of the nonuniformity of growth and remodeling (7). A recent study (22) reported that flow overload induced growth of adventitia that exceeded that of intima and, hence, decreased the opening angle. The opening angle was found to be increased in hypertension (6). The present data show that the opening angle of coronary artery was decreased after long-term exposure of CS (Fig. 7). This suggests that the growth of adventitia exceeds that of intima or that the intima resorbs more than the adventitia. This is in contrast to the pulmonary arteries that are in more direct contact with the products of smoke (21).

Uniform Strain and Stress Hypothesis

It is well accepted that a homeostatic state of stress exists in the cardiovascular system. Our laboratory (9) has recently found that the strain (computed in reference to the zero-stress state) is very uniform along the cardiovascular system, i.e., from small to large vessels. We also found that in hypertension or flow overload where the homeostatic wall strain is suddenly altered, the vessel will remodel (including the zero-stress state) in such a way as to normalize the wall strain and restore mechanical homeostasis (5, 22). Here we show that CS markedly decreased the circumferential strain and stress in coronary artery. The strain was decreased by ~19% to 25%, and the stress was decreased by ~9% to 12% in response to CS. Moreover, this change in stress and strain was irreversible after cessation of CS exposure for the two groups (Fig. 5). These findings reflect a change of mechanical homeostasis of vessel wall and possibly function.

Correlation Between NO and Structural and Mechanical Properties

NO appears to be intimately connected with vessel wall structure and mechanical properties (16, 30). Here we report a significant relationship between the NO bioavailability (nitrite) and the structural and mechanical properties as shown in Fig. 8. The stress and strain show a significant linear relation, whereas the WT and modulus reveal an inverse relation. Although the data on mechanical properties and nitrite concentration stemmed from different arteries in this study, we have confirmed that there existed a linear relation for NO byproducts between coronary and combined femoral and carotid arteries in mice ($R^2 = 0.79$, $P < 0.05$). Our results demonstrated that the reduction of NO production by CS may be responsible, at least in part, for the increased intima-medial thickness and arterial stiffness of coronary arteries.

The present data provide a basis for future mechanistic investigations of the interactions between NO and the mechanical properties of the vessel. For example, is the dysfunction in NO synthesis the cause of the mechanical remodeling on the mouse arteries? This and other questions may be assessed by pharmacological blockers and transgenic models in future studies.

In summary and in conclusion, the present study demonstrates that CS has an immediate and substantial effect on structural and elastic properties of mouse coronary arteries which highly correlated with a decrease in NO bioavailability. Moreover, long-term CS exposure can cause an irreversible deterioration of structural and elastic properties of coronary arteries. The decrease in NO bioavailability in vessel wall stiffness may explain why CS is an important risk factor for coronary artery disease. The observed recovery of NO bioavailability after short-term, but not long-term, smoke cessation is an important public health message.

ACKNOWLEDGMENTS

We thank Deniz Ari for exposure of mice to cigarette smoke.

GRANTS

This research was supported in part by the National Heart, Lung, and Blood Institute Grant 2-R01-HL055554-06 and by a University of California, Irvine, Transdisciplinary Tobacco Use Research Center award.

REFERENCES

1. **Auerbach O and Garfinkel L.** Atherosclerosis and aneurysm of the aorta in relation to smoking habit and age. *Chest* 78: 805–809, 1980.
2. **Barua RS, Ambrose JA, Eales-Reynolds LJ, DeVoe MC, Zervas JG, and Saha DC.** Dysfunctional endothelial nitric oxide biosynthesis in healthy smokers with impaired endothelium-dependent vasodilatation. *Circulation* 104: 1905–1910, 2001.
3. **Bogren HG, Mohiaddin RH, Klipstein RK, Firmin DN, Underwood RS, Rees SR, and Longmore DB.** The function of the aorta in ischemic heart disease: a magnetic resonance and angiographic study of aortic compliance and blood flow patterns. *Am Heart J* 118: 234–247, 1989.
4. **Chalon S, Moreno H, Benowitz NL, Hoffman BB, and Blaschke TF.** Nicotine impairs endothelium-dependent dilatation in human veins in vivo. *Clin Pharmacol Ther* 67: 391–397, 2000.

5. **Duch BU, Andersen HL, Smith J, Kassab GS, and Gregersen H.** Structural and mechanical remodeling of the common bile duct during experimental obstruction. *Neurogastroenterol Motil* 14: 111–122, 2002.
6. **Fung YC and Liu SQ.** Change of zero-stress state of rat pulmonary arteries in hypoxic hypertension. *J Appl Physiol* 262: 2455–2470, 1992.
7. **Fung YC.** *Biomechanics: Motion, Flow, Stress, and Growth.* New York: Springer-Verlag, 1990.
8. **Groppelli A, Omboni S, Parati G, and Mancia G.** Blood pressure and heart rate response to repeated smoking before and after P-blockade and selective a, inhibition. *J Hypertens Suppl* 8: s35–s40, 1990.
9. **Guo X and Kassab GS.** Distribution of stress and strain along the porcine aorta and coronary arterial tree. *Am J Physiol Heart Circ Physiol* 286: H2361–H2368, 2004.
10. **Guo X and Kassab GS.** Variation of mechanical properties along the length of the aorta in C57bl/6 mice. *Am J Physiol Heart Circ Physiol* 285: H2614–H2622, 2003.
11. **Higman DJ, Strachan AM, Buttery L, Hicks RC, Springall DR, Greenhalgh RM, and Powell JT.** Smoking impairs the activity of endothelial nitric oxide synthase in saphenous vein. *Arterioscler Thromb Vasc Biol* 16: 546–552, 1996.
12. **Hoffman D and Wynder EL.** Chemical constituents and bioactivity of tobacco smoke. In: *Tobacco, A Major International Health Hazard*, edited by Zaridge DG and Peto R. London: International Agency for Research on Cancer, World Health Organization, Oxford University Press, 145–165, 1986.
13. **Houdi AA, Dowell RT, and Diana JN.** Cardiovascular responses to cigarette smoke exposure in restrained conscious rats. *J Pharmacol Exp Ther* 275: 646–653, 1995.
14. **Ignarro LJ, Buga GM, Wood KS, Byrns RE, and Chaudhuri G.** Endothelium-derived relaxing factor produced and released from artery and vein is nitric oxide. *Proc Natl Acad Sci USA* 84: 9265–9269, 1987.
15. **Kannel WB, McGee D, and Castelli WP.** Latest perspective on cigarette smoking and cardiovascular disease: the Framingham Study. *J Cardiac Rehabil* 4: 267–277, 1984.
16. **Kinlay S, Creager MA, Fukumoto M, Hikita H, Fang JC, Selwyn AP, and Ganz P.** Endothelium-derived nitric oxide regulates arterial elasticity in human arteries in vivo. *Hypertension* 38: 1049–1053, 2001.
17. **Kiowski W, Linder L, Stoschitzky K, Pfisterer M, Burckhardt D, Burkart F, and Buhler FR.** Diminished vascular response to inhibition of endothelium-derived nitric oxide and enhanced vasoconstriction to exogenously administered endothelin-1 in clinically healthy smokers. *Circulation* 90: 27–34, 1994.
18. **Kool MJ, Hoeks AP, Boudier HA, Reneman RS, and Van Bortel LM.** Short- and long-term effects of smoking on arterial wall properties in habitual smokers. *J Am Coll Cardiol* 22: 1881–1886, 1993.
19. **Kugiyama K, Yasue H, Ohgushi M, Motoyama T, Kawano H, Inobe Y, Hirashima O, and Sugiyama S.** Deficiency in nitric oxide bioactivity in epicardial coronary arteries of cigarette smokers. *J Am Coll Cardiol* 28: 1161–1167, 1996.
20. **Laing SP, Greenhalgh RM, and Taylor GW.** The prevalence of cigarette smoking in patients with arterial disease. In: *Smoking and Arterial Disease*, edited by Greenhalgh RM. London: Pitman Medical, 1981.
21. **Liu SQ and Fung YC.** Changes in the structure and mechanical properties of pulmonary arteries of rats exposed to cigarette smoke. *Am Rev Respir Dis* 148: 768–777, 1993.
22. **Lu X, Zhao JB, Wang GR, Gregersen H, and Kassab GS.** Remodeling of the zero-stress state of the femoral artery in response to flow overload. *Am J Physiol Heart Circ Physiol* 280: H1547–H1559, 2001.
23. **Lu X and Kassab GS.** Nitric oxide is significantly reduced in ex vivo porcine arteries during reverse flow because of increased superoxide production. *J Physiol* 561: 575–582, 2004.
24. **Moncada S and Higgs A.** The L-arginine-nitric oxide pathway. *N Engl J Med* 329: 2002–2012, 1993.
25. **Oemar BS, Tschudi MR, Godoy N, Brovkovich V, Malinski T, and Luscher TF.** Reduced endothelial nitric oxide synthase expression and production in human atherosclerosis. *Circulation* 97: 2494–2498, 1998.
26. **Powell JT and Higman DJ.** Smoking, nitric oxide and the endothelium. *Br J Surg* 81: 785–787, 1994.
27. **Rees DD, Palmer RM, and Moncada S.** Role of endothelium-derived nitric oxide in the regulation of blood pressure. *Proc Natl Acad Sci USA* 86: 3375–3378, 1989.
28. **Scott-Burden T and Vanhoutte PM.** The endothelium as a regulator of vascular smooth muscle proliferation. *Circulation* 87, *Suppl* V: V51–V55, 1993.
29. **Stefanadis C, Vlachopoulos C, Tsiamis E, Diamantopoulos L, Toutouzas K, and Giatrakos N.** Unfavourable effects of passive smoking on aortic function in men. *Ann Intern Med* 128: 426–434, 1998.
30. **Stewart JM, Xu X, Ochoa M, and Hintze TH.** Exercise reduces epicardial coronary artery wall stiffness: roles of cGMP and cAMP. *Med Sci Sports Exerc* 30: 220–228, 1998.
31. **Su Y, Han W, Giraldo C, De Li Y, and Block ER.** Effect of cigarette smoke extract on nitric oxide synthase in pulmonary artery endothelial cells. *Am J Respir Cell Mol Biol* 19: 819–825, 1998.
32. **Tani S, Dimayuga PC, Anazawa T, Chyu KY, Li H, Shah PK, and Cercek B.** Aberrant antibody responses to oxidized LDL and increased intimal thickening in apoE$^{-/-}$ mice exposed to cigarette smoke. *Atherosclerosis* 175: 7–14, 2004.
33. **Trachtman H, Futterweit S, Garg P, Reddy K, and Singhal PC.** Nitric oxide simulates the activity of a 712-kDa neutral matrix metalloproteinase in cultured rat mesangial cells. *Biochem Biophys Res Commun* 218: 704–708, 1996.
34. **Ueda S, Matsuoka H, Miyazaki H, Usui M, Okuda S, and Imaizumi T.** Tetrahydrobiopterin restores endothelial function in long-term smokers. *J Am Coll Cardiol* 35: 71–75, 2000.
35. **Wang H, Ye Y, Zhu M, and Cho C.** Increased interleukin-8 expression by cigarette smoke extract in endothelial Cells. *Environ Toxicol Pharmacol* 9: 19–23, 2000.